

**The relationship  
between Arabian Sea  
upwelling and Indian  
monsoon revisited**

X. Yi et al.

# The relationship between Arabian Sea upwelling and Indian monsoon revisited

**X. Yi, B. Hünicke, N. Tim, and E. Zorita**

Helmholtz-Zentrum Geesthacht, Institute of Coastal Research, Max-Planck-Str.1,  
21502 Geesthacht, Germany

Received: 10 September 2015 – Accepted: 20 October 2015 – Published: 6 November 2015

Correspondence to: X. Yi (xing.yi@hzg.de)

Published by Copernicus Publications on behalf of the European Geosciences Union.

Title Page

Abstract

Introduction

Conclusions

References

Tables

Figures



Back

Close

Full Screen / Esc

Printer-friendly Version

Interactive Discussion









sources. SST data are obtained from the Advanced Very High Resolution Radiometer (AVHRR) Pathfinder Version 5.0 (Casey et al., 2010). Wind data are provided by the NCEP/NCAR reanalysis and the Cross-Calibrated Multi-Platform (CCMP) project (Atlas et al., 2011). The along-shore upwelling favorable wind-stress is calculated as:

$$\tau_{SW} = \rho \times C_D \times \sqrt{u^2 + v^2} \times (u / \cos \alpha + v / \cos \beta)$$

where  $\rho$  is the air density which is assumed as  $1.22 \text{ kg m}^{-3}$  and the drag coefficient  $C_D$  is computed using the formulation of Yelland and Taylor (1996);  $u$  and  $v$  are the zonal (eastward) and meridional (northward) wind speed components respectively;  $\alpha$  and  $\beta$  are the angles between the along-shore direction and the wind speed components and in this case both of them are assumed to  $45^\circ$  because in our study the upwelling favorable wind-stress is from the direction of southwest (SW).

In order to estimate the relationship between upwelling and the monsoon, we employ the Indian monsoon index (IMI) defined by Wang and Fan (1999) and the all India monsoon rainfall index (IMR) from the Indian Institute of Tropical Meteorology (Parthasarathy et al., 1994) as well as the Webster and Yang monsoon index (WYM) defined by Webster and Yang (1992). We calculate the IMI and WYM based on wind speed from NCEP/NCAR reanalysis while the IMR is obtained from station rainfall records in India. Besides, several other meteorological and oceanic variables are also investigated. Air temperature data produced by University of Delaware (Willmott and Matsuura, 2012) and sea level pressure (SLP) data from the NCEP/NCAR reanalysis are investigated to provide further understanding. Because of a continuity issue in the STORM simulation output (missing data in 1949), we limit the study period from 1950 to 2010. All data share the same temporal coverage except the period covered by SST data from AVHRR from 1985 to 2009, the wind from CCMP covers from 1988 to 2010, and the IMR is from 1950 to 2000.

## The relationship between Arabian Sea upwelling and Indian monsoon revisited

X. Yi et al.

Title Page

Abstract

Introduction

Conclusions

References

Tables

Figures

◀

▶

◀

▶

Back

Close

Full Screen / Esc

Printer-friendly Version

Interactive Discussion



### 3 Coastal upwelling in the western Arabian Sea

Upwelling along the west coast of the Arabian Sea usually starts in May and ends in September (Brock et al., 1991). This is well reproduced in the modeled annual cycle of the upwelling velocity (Fig. 1a), which is converted from the original model output of upward water mass transport. Thus, positive values indicate upwelling whereas negative values indicate downwelling. The upwelling velocity annual cycle shows that the significant positive values start from May, peak in July and end in September. As one of the traditional upwelling indices, the SW wind-stress (Fig. 1b) is in good consistency with the upwelling velocity with a peak in July as well. Another traditional upwelling index is the observed coastal SST and our modeled SST (Fig. 1c) also reveals good correlation with the upwelling velocity with a lag of approximately one month. This lag can be explained by the time needed to transport deeper and cooler water to the surface and it matches a similar lag between wind-stress and SST found in the observations by Rixen et al. (2000). It is obvious that the ranges of these three annual cycles tend to get larger when the upwelling becomes stronger. Therefore, unless indicated otherwise, we average the values from June to August (JJA) for upwelling velocity and SW wind-stress in the following analyses and we select July to September (JAS) for SST due to the mentioned lag.

The coastal upwelling domain in this study (Fig. 1d) is chosen from 15.2 to 22.3° N along the coast of Yemen and Oman with an expansion of ~ 90 km (Rixen et al., 2000). According to Brock and McClain (1992), we average the upwelling velocity over the upper 200 m of water. This selected coastal band is very narrow but with the advantage from the high resolution of the STORM simulation we are able to observe the spatial patterns of the upwelling in the study domain. The simulated mean upwelling velocity averaged over this domain in JJA from 1950 to 2010 is about 1.8 m day<sup>-1</sup>. Upwelling is less intense in the area north to Ras Madrasah and much stronger at regions near the capes such as Sawqirah and Nishtun where the velocity can exceed 6 m day<sup>-1</sup>.

OSD

12, 2683–2704, 2015

## The relationship between Arabian Sea upwelling and Indian monsoon revisited

X. Yi et al.

Title Page

Abstract

Introduction

Conclusions

References

Tables

Figures



Back

Close

Full Screen / Esc

Printer-friendly Version

Interactive Discussion



## 4 Upwelling variability

For an understanding about the spatial variability of upwelling in this region, we calculate the standard deviation (SD) and perform an Empirical Orthogonal Function (EOF) analysis (von Storch and Zwiers, 2001) of the upwelling velocity. The SD map (Fig. 2a) shows that higher intensity of upwelling comes with higher variance, that is, in the regions where the upwelling velocity is higher (Fig. 1d), the SD of the upwelling velocity is also higher. The mean SD over the entire study area is about  $0.7 \text{ m day}^{-1}$ , which is nearly half of the mean upwelling velocity. The EOF analysis is a method that identifies the main spatial patterns of coherent variation. This method identifies spatial patterns, uncorrelated, in time, that describe most of the data variance. The first EOF mode explains most of the variance, which represents the most apparent variation in the data. In our case the leading mode arising from the EOF analysis (Fig. 2b) reveals apparent coastal-offshore pattern and accounts for 10 % of the total variance. The first principal component (PC1) time series is highly consistent with the spatially averaged upwelling velocity ( $r = 0.82$ , shown in Fig. 3b). However, the high SD with respect to the mean value of upwelling velocity and the low explained variance from the first mode of the EOF analysis together indicate that the upwelling in this region is affected by various and complex processes.

Beside the spatial variability, the temporal variability of upwelling is studied as well. The primary attempt is to detect a trend in the upwelling time series referring to the Bakun hypothesis (Bakun, 1990) that upwelling intensification appears at global scale. However, only a negligible increasing trend is revealed over the last 61 years (Fig. 3a). This trend has a slope of  $0.0035 \text{ m day}^{-1} \text{ year}^{-1}$ , which is only 0.2% of the mean coastal upwelling velocity in the domain. Hence, it is concluded that no detectable trend can be found in our upwelling velocity and thus we do not further discuss about trends in the following text. To make sure all the variables are comparable with each other, we remove the trends in all of them for further analyses.

OSD

12, 2683–2704, 2015

### The relationship between Arabian Sea upwelling and Indian monsoon revisited

X. Yi et al.

Title Page

Abstract

Introduction

Conclusions

References

Tables

Figures



Back

Close

Full Screen / Esc

Printer-friendly Version

Interactive Discussion



## The relationship between Arabian Sea upwelling and Indian monsoon revisited

X. Yi et al.

Title Page

Abstract

Introduction

Conclusions

References

Tables

Figures

◀

▶

◀

▶

Back

Close

Full Screen / Esc

Printer-friendly Version

Interactive Discussion



We compare the time series of the upwelling velocity with SST and the SW wind-stress to validate our modeled upwelling data since they are generally applied as coastal upwelling indices (Fig. 3b–d). The time series of upwelling and SST are generated using data within the upwelling domain shown in Fig. 1d while the SW wind-stress time series contains data from a broader area due to the low resolution of the wind data. In Fig. 3b, the upwelling velocity and the PC1 time series from the EOF analysis are compared with SST from the STORM simulation and the SW wind-stress from the NCEP/NCAR reanalysis. The comparison reveals that the upwelling is strongly negatively correlated to the SST ( $r = -0.83$ ) as well as positively to the SW wind-stress ( $r = 0.73$ ).

Since the SST and the upwelling velocity are both outputs from the STORM simulation and the NCEP wind data is the forcing used in this simulation, these high correlations are to some extent expected and less persuasive without the support from extra sources. Therefore, we employ wind data from CCMP and SST data from AVHRR (Fig. 3c and d) as they are independent of the STORM simulation, although their temporal coverages are shorter than STORM. The correlations between simulated upwelling and these two observed variables are lower (wind  $r = 0.49$  and SST  $r = -0.45$ ) but they remain significant at the 95 % level or higher as in the previous analysis. These results suggest that the upwelling velocity derived from the STORM simulation is significantly consistent with the traditional upwelling indices so it is reasonable to use it for further studies such as investigating the responsible processes affecting the upwelling.

### 5 Link to the Monsoon

As the ISM has been suggested to be strongly linked to the western Arabian Sea upwelling, we examine the relationship between the simulated upwelling velocity and the monsoon indices Indian monsoon index (IMI), all India monsoon rainfall index (IMR) and the Webster and Yang monsoon index (WYM) in Fig. 4. Note that the IMR is computed by integrating the total rainfall records of numerous stations from June to

## The relationship between Arabian Sea upwelling and Indian monsoon revisited

X. Yi et al.

Title Page

Abstract

Introduction

Conclusions

References

Tables

Figures



Back

Close

Full Screen / Esc

Printer-friendly Version

Interactive Discussion



September (JJAS) and the data source is not available for single months. Thus, we calculate the IMI and the WYM and also the upwelling velocity for the extended JJAS season. All of the three comparisons show low and negative correlations in the northern part of the domain. Higher correlations are found along the coast and to the south especially the regions with more intense upwelling and larger variance, but only a few areas show correlations that pass the significance level of 95 %.

One interesting finding is that the correlation patterns obtained with IMI (Fig. 4a) and with IMR (Fig. 4b) are quite similar. The correlations start to become positive at Ras Madrasah and the highest and the most significant correlations are located between Sawqirah and Nishtun. Besides, the areas with stronger correlation and higher significance highly overlap. Considering the fact that IMI is calculated from the difference of two SLP fields whereas IMR is obtained from the rainfall records, this similarity indicates that the upwelling has very similar link to the variation of the SLP and the rainfall. However, the WYM correlation pattern (Fig. 4c) shows a different case where the positive values begin to appear from the north of Ras Madrasah and the strongest and most significant correlation lies between Ras Madrasah and Nishtun. Although WYM is also calculated from the difference of two SLP fields, the strategies for selecting the SLP fields are not the same and this is causing the difference between the patterns of IMI and WYM. Additionally, as the SLP-based indices, IMI and WYM patterns capture reduced correlations near Salalah but IMR does not.

The spatially heterogeneous correlations indicate that the upwelling velocities in different regions along the western Arabian Sea coast are sensitive to different forcing mechanisms. Furthermore, it is surprising that the overall correlations of upwelling with all monsoon indices are rather low and insignificant. This analysis, therefore, indicates that the impact of the ISM on western Arabian Sea coastal upwelling is weak and limited to areas with upwelling of higher intensity (Fig. 1d) and variability (Fig. 2a).

## 6 SLP and Monsoon

In order to determine the other possible forcings that could influence the variability of upwelling, we correlate the PC1 time series of upwelling to SLP and air temperature in the broader Asian (Indian Ocean) region. As the first principal component time series from the EOF analysis, PC1 captures the major variation of the upwelling velocity. In Fig. 5a, the correlation between PC1 and SLP is shown in the background contour, while the two-dimensional correlation with wind is superimposed on it. Positive correlation to SLP is found in the Arabian Sea and negative correlation over the Himalayas. The areas with the strongest positive and negative correlations are within the regions used for calculating the IMI. We take one box from the highest positive correlation area and one box from the highest negative correlation area. The SLP gradient between these two areas boxes presents a strong correlation with averaged upwelling PC1 ( $r = 0.68$ ). This is also evidenced in the correlation between the upwelling PC1 and the wind speed vectors. It is obvious that the upwelling PC1 is significantly correlated to the southwestern wind in the Arabian Sea as a result of the gradient of SLP. Furthermore, along the western coast where the upwelling exists, the connection with the southwestern wind is the strongest.

Also importantly, Fig. 5b reveals a link between the upwelling PC1 and the surface air temperature. The upwelling PC1 is positively correlated to the air temperature over the Tibetan Plateau and negatively correlated to that over northern India. Both correlations are significant and similar to the study with the SLP field we select two boxes from the air temperature field as well. The correlation between the upwelling PC1 and the gradient of these two regions is also not negligible ( $r = 0.49$ ). The links between the upwelling PC1 and SLP as well as the air temperature imply that other factors also affect upwelling.

Finally, we correlate the monsoon indices with the SLP field to gain a better understanding about their different influences on the upwelling. Same as the analysis of the correlation between upwelling and the monsoon indices, we extend the selected period

OSD

12, 2683–2704, 2015

### The relationship between Arabian Sea upwelling and Indian monsoon revisited

X. Yi et al.

Title Page

Abstract

Introduction

Conclusions

References

Tables

Figures



Back

Close

Full Screen / Esc

Printer-friendly Version

Interactive Discussion







*Acknowledgements.* This work is funded by the Cluster of Excellence Integrated Climate System Analysis and Prediction (CliSAP) Project B3. We thank the Max-Planck-Institute for Meteorology for providing the model data. All the other publicly available data used in this study are gratefully acknowledged.

The article processing charges for this open-access publication were covered by a Research Centre of the Helmholtz Association.

## References

- Anderson, D. M., Brock, J. C., and Prell, W. L.: Physical upwelling processes, upper ocean environment and the sediment record of the southwest monsoon, Geological Society, London, Special Publications, 64, 121–129, 1992.
- Anderson, D. M., Overpeck, J. T., and Gupta, A. K.: Increase in the Asian southwest monsoon during the past four centuries, *Science*, 297, 596–599, 2002.
- Atlas, R., Hoffman, R. N., Ardizzone, J., Leidner, S. M., Jusem, J. C., Smith, D. K., and Gombos, D.: A cross-calibrated multiplatform ocean surface wind velocity product for meteorological and oceanographic applications, *B. Am. Meteorol. Soc.*, 92, 157–174, 2011.
- Bakun, A.: Coastal Upwelling Indices, West Coast of North America, 1946–71, NOAA Tech. Rep., 1973, 103, US Department of Commerce, National Oceanic and Atmospheric Administration, National Marine Fisheries Service, 1973.
- Bakun, A.: Global climate change and intensification of coastal ocean upwelling, *Science*, 247, 198–201, 1990.
- Banzon, V. F., Evans, R. E., Gordon, H. R., and Chomko, R. M.: SeaWiFS observations of the Arabian Sea southwest monsoon bloom for the year 2000, *Deep-Sea Res. Pt. II*, 51, 189–208, 2004.
- Brock, J. C. and McClain, C. R.: Interannual variability in phytoplankton blooms observed in the northwestern Arabian Sea during the Southwest Monsoon, *J. Geophys. Res.-Oceans*, 97, 733–750, 1992.
- Brock, J. C., McClain, C. R., Luther, M. E., and Hay, W. W.: The phytoplankton bloom in the northwestern Arabian Sea during the Southwest Monsoon of 1979, *J. Geophys. Res.-Oceans*, 96, 20623–20642, 1991.

## The relationship between Arabian Sea upwelling and Indian monsoon revisited

X. Yi et al.

Title Page

Abstract

Introduction

Conclusions

References

Tables

Figures



Back

Close

Full Screen / Esc

Printer-friendly Version

Interactive Discussion





## The relationship between Arabian Sea upwelling and Indian monsoon revisited

X. Yi et al.

[Title Page](#)[Abstract](#)[Introduction](#)[Conclusions](#)[References](#)[Tables](#)[Figures](#)[Back](#)[Close](#)[Full Screen / Esc](#)[Printer-friendly Version](#)[Interactive Discussion](#)

Ma, J. F., Liu, H. L., Lin, P. F., and Zhan, H. G.: Seasonality of biological feedbacks on sea surface temperature variations in the Arabian Sea: the role of mixing and upwelling, *J. Geophys. Res.-Oceans*, 119, 7592–7604, 2014.

Manghnani, V., Morrison, J. M., Hopkins, T. S., and Bohm, E.: Advection of upwelled waters in the form of plumes off Oman during the Southwest Monsoon, *Deep-Sea Res. Pt. II*, 45, 2027–2052, 1998.

Naik, S. S., Godad, S. P., Naidu, P. D., and Ramaswamy, V.: A comparison of Globigerinoides ruber calcification between upwelling and non-upwelling regions in the Arabian Sea, *J. Earth Syst. Sci.*, 122, 1153–1159, 2013.

Narayan, N., Paul, A., Mulitza, S., and Schulz, M.: Trends in coastal upwelling intensity during the late 20th century, *Ocean Sci.*, 6, 815–823, doi:10.5194/os-6-815-2010, 2010.

Parthasarathy, B., Munot, A. A., and Kothawale, D. R.: All-India monthly and seasonal rainfall series – 1871–1993, *Theor. Appl. Climatol.*, 49, 217–224, 1994.

Prell, W. L. and Curry, W. B.: Faunal and isotopic indexes of monsoonal upwelling – western Arabian Sea, *Oceanol. Acta*, 4, 91–98, 1981.

Prell, W. L. and Vancampo, E.: Coherent response of Arabian Sea upwelling and pollen transport to Late Quaternary Monsoonal winds, *Nature*, 323, 526–528, 1986.

Rao, A. D., Joshi, M., and Ravichandran, M.: Oceanic upwelling and downwelling processes in waters off the west coast of India, *Ocean Dynam.*, 58, 213–226, 2008.

Rixen, T., Haake, B., and Ittekkot, V.: Sedimentation in the western Arabian Sea the role of coastal and open-ocean upwelling, *Deep-Sea Res. Pt. II*, 47, 2155–2178, 2000.

Shi, W., Morrison, J. M., Bohm, E., and Manghnani, V.: The Oman upwelling zone during 1993, 1994 and 1995, *Deep-Sea Res. Pt. II*, 47, 1227–1247, 2000.

Tozuka, T., Nagura, M., and Yamagata, T.: Influence of the reflected Rossby waves on the western Arabian Sea upwelling region, *J. Phys. Oceanogr.*, 44, 1424–1438, 2014.

von Storch, H. and Zwiers, F. W.: *Statistical Analysis in Climatic Research*, Cambridge University Press, Cambridge, UK, 484 pp., 2001.

von Storch, J.-S., Eden, C., Fast, I., Haak, H., Hernández-Deckers, D., Maier-Reimer, E., Marotzke, J., and Stammer, D.: An estimate of the Lorenz energy cycle for the world ocean based on the STORM/NCEP simulation, *J. Phys. Oceanogr.*, 42, 2185–2205, 2012.

Wang, B. and Fan, Z.: Choice of south Asian summer monsoon indices, *B. Am. Meteorol. Soc.*, 80, 629–638, 1999.



## The relationship between Arabian Sea upwelling and Indian monsoon revisited

X. Yi et al.

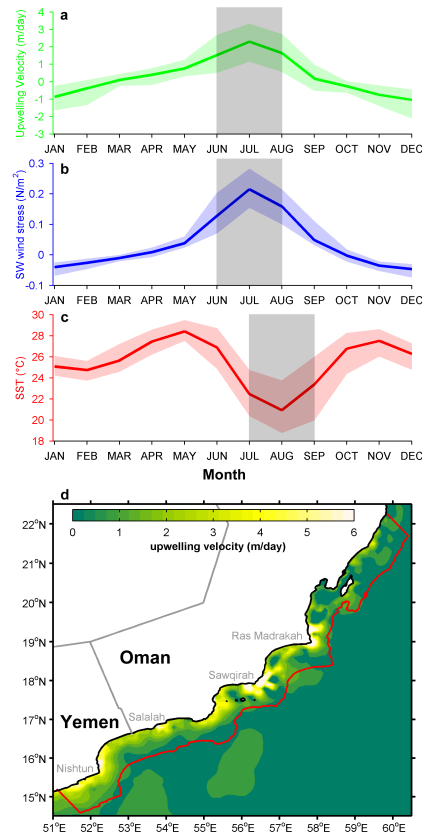


**Figure 1.** Annual cycle of (a) upwelling velocity, (b) SW wind-stress and (c) sea-surface temperature averaged for the study area. Color shaded areas are the ranges of the annual cycles and grey shaded months are the study periods selected for each variable. (d) JJA mean upwelling velocity from 1950 to 2010. The red contour demonstrates the study area.

## The relationship between Arabian Sea upwelling and Indian monsoon revisited

X. Yi et al.

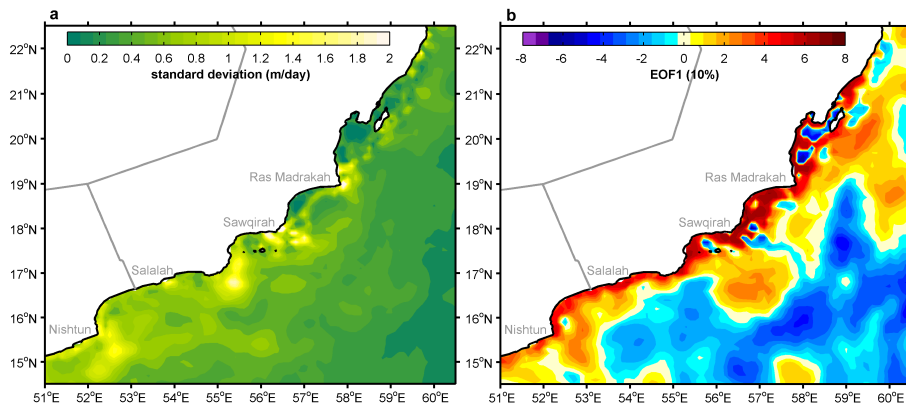


**Figure 2.** (a) Standard deviation of JJA upwelling velocity from 1950 to 2010. (b) First mode of the EOF analysis with its explained variance in parentheses.

[Title Page](#)[Abstract](#)[Introduction](#)[Conclusions](#)[References](#)[Tables](#)[Figures](#)[◀](#)[▶](#)[◀](#)[▶](#)[Back](#)[Close](#)[Full Screen / Esc](#)[Printer-friendly Version](#)[Interactive Discussion](#)

## The relationship between Arabian Sea upwelling and Indian monsoon revisited

X. Yi et al.

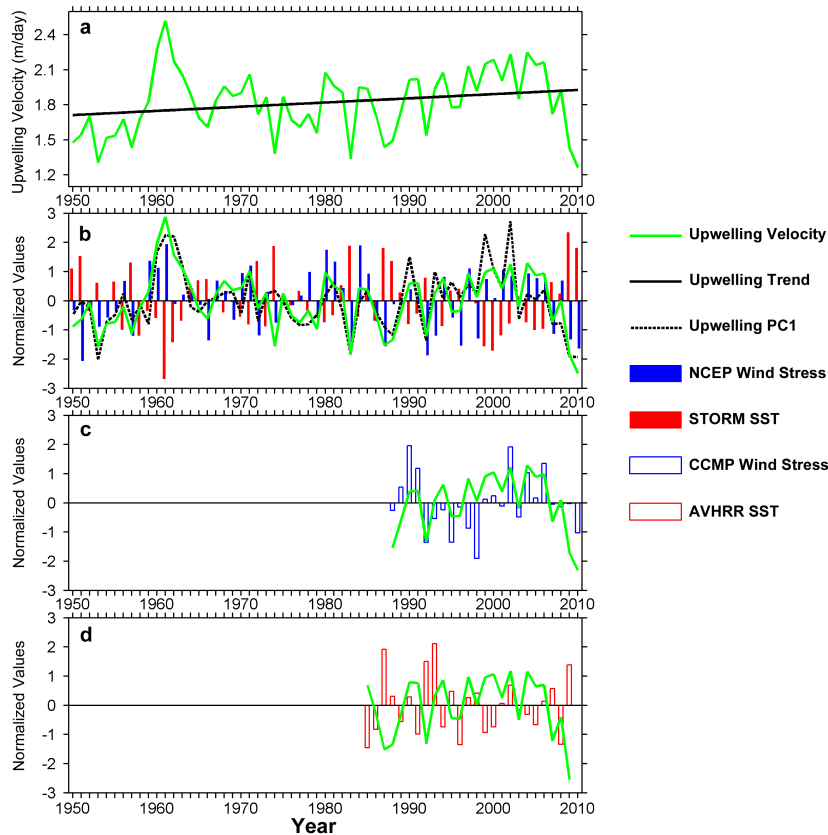


**Figure 3.** (a) Time series of upwelling velocity and its long term trend. (b) Comparison of upwelling velocity, upwelling PC1, SW wind-stress from NCEP and SST from STORM. (c) Upwelling velocity and SW wind-stress from CCMP. (d) Upwelling velocity and SST from AVHRR. All the time series in (b), (c) and (d) are detrended and normalized.

[Title Page](#)
[Abstract](#)
[Introduction](#)
[Conclusions](#)
[References](#)
[Tables](#)
[Figures](#)
[Back](#)
[Close](#)
[Full Screen / Esc](#)
[Printer-friendly Version](#)
[Interactive Discussion](#)

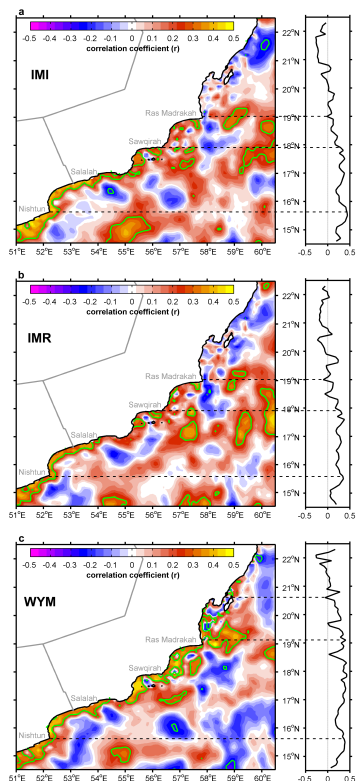


**Figure 4.** Correlation between upwelling velocity and **(a)** IMI, **(b)** IMR as well as **(c)** WYM indices. Within the green contours are the areas where the significant levels are 95 % or higher. The plots on the right column are the meridional mean correlation coefficient between upwelling velocity and each monsoon index averaged within the study area. The upper dashed line indicates the general starting points of the positive correlation. Between the middle and the lower dashed lines are the areas where the correlations are the highest.

**The relationship between Arabian Sea upwelling and Indian monsoon revisited**

X. Yi et al.

Title Page

Abstract Introduction

Conclusions References

Tables Figures

◀ ▶

◀ ▶

Back Close

Full Screen / Esc

Printer-friendly Version

Interactive Discussion



## The relationship between Arabian Sea upwelling and Indian monsoon revisited

X. Yi et al.

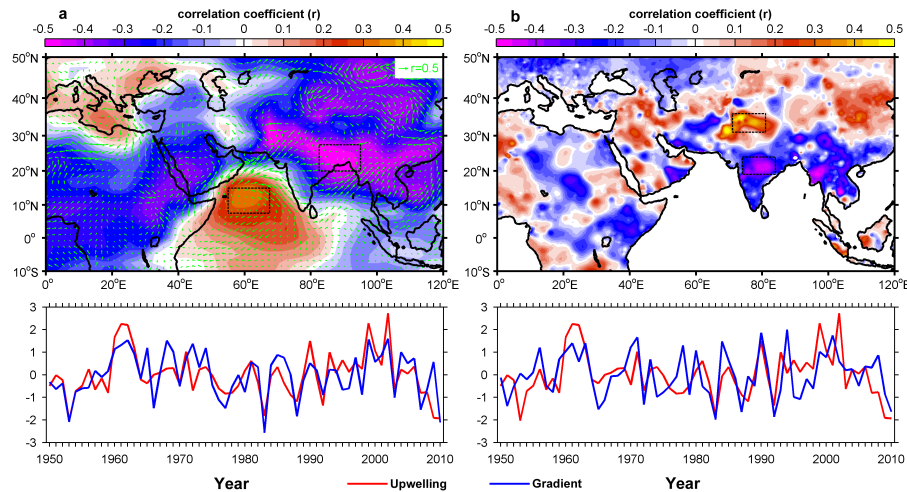


**Figure 5.** (a) Correlation between upwelling PC1 and SLP is represented by the background color contour. Green arrows are the two-dimensional correlation between upwelling velocity and the wind speed. (b) Background color contour is the correlation between upwelling PC1 and the air temperature. The lower plots are the time series of the PC1 and the corresponding time series of the gradient between the two selected boxes in the upper maps. The two plots are detrended and normalized.

## The relationship between Arabian Sea upwelling and Indian monsoon revisited

X. Yi et al.

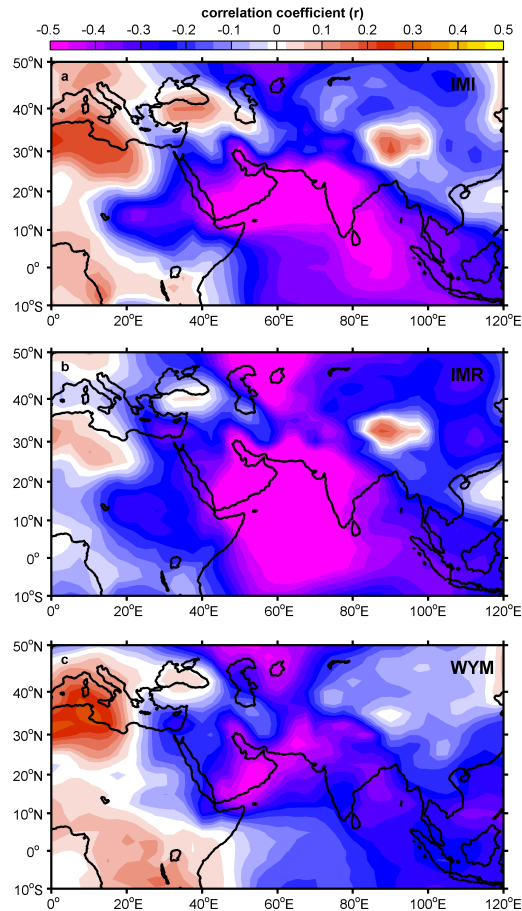


**Figure 6.** Correlations between SLP and the monsoon indices: **(a)** IMI, **(b)** IMR and **(c)** WYM.

[Title Page](#)[Abstract](#)[Introduction](#)[Conclusions](#)[References](#)[Tables](#)[Figures](#)[◀](#)[▶](#)[◀](#)[▶](#)[Back](#)[Close](#)[Full Screen / Esc](#)[Printer-friendly Version](#)[Interactive Discussion](#)